

Classical trajectories of molecules exposed to few-optical-cycle light pulses

S. Stagira,* G. Sansone, C. Vozzi, and M. Nisoli

National Laboratory for Ultrafast and Ultraintense Optical Science, CNR-INFN, Dipartimento di Fisica, Politecnico Piazza L. da Vinci 32, I-20133 Milano, Italy

(Received 20 December 2004; revised manuscript received 19 December 2005; published 7 April 2006)

It is shown that, in the framework of classical electrodynamics and in some peculiar cases, an exhaustive description of rotational evolution of molecules driven by intense few-optical-cycle laser pulses should consider the electric field of the pulse rather than its intensity envelope. We show that, at moderate pulse intensities, nonlinear effects driven by the molecular hyperpolarizability play a significant role. These findings are illustrated by numerical simulations concerning the classical motion of several molecules exposed to few-cycle light pulses.

DOI: [10.1103/PhysRevA.73.043403](https://doi.org/10.1103/PhysRevA.73.043403)

PACS number(s): 32.80.Lg, 42.65.Re

I. INTRODUCTION

Classical theories concerning the motion of microscopic polarizable bodies in electric fields have been developed a long time ago, as proven by the pioneering work of Debye about the orientation of polar molecules in a static field [1,2]. Beyond the academic interest, the classical description of molecular dynamics driven by electromagnetic waves is a helpful tool in the understanding of many physical phenomena; among many examples, we could recall the classical interpretation of the slow nonlinear optical response in gases [3] and liquids [4] and the classical description of anisotropy in molecular photodissociation [5,6].

As a matter of fact, a complete and exhaustive description of molecular rotational motion can be achieved only in the framework of a quantum theory [7]. Nevertheless, owing to the clear insight that a classical description provides and to the larger computational costs required by quantum models, the comparative study of classical against quantum molecular dynamics has acquired strong importance in the past [8] and it is nowadays still active today [9,10]. The fundamental reason for the strong interest in this topic is that laser-induced molecular alignment [11,12] is nowadays an important investigation tool in molecular physics [13]. This effect has been exploited in the study [14] and the applications [15,16] of impulsive rotational Raman scattering; it can be used for the implementation of molecular trapping [17]; it allows the investigation of high-order harmonic generation as a function of molecular alignment [18–20]; it can provide useful insight into the physics of chemical reactions [21] and in chemical bond dissociation of molecules [22–24].

A large number of theoretical models, describing nonresonant laser-molecule interaction, are based on the general assumption that the molecular response time is very large in comparison to the optical period; it is worth noting that, in the literature, such assumption is shared by quantum and classical models. In this approximation the laser pulse envelope acts as the driving term and the rapid oscillations of the electric field are neglected. Moreover, in the case of polar

molecules, the presence of a permanent dipole moment has negligible effects on the final state of the molecule. A further common assumption is that the nonlinear contributions to the induced molecular dipole moment do not play any role in the molecular dynamics. Hereafter, the ensemble of these assumptions will be called *linear envelope approximation* (LEA).

In a broad range of interaction conditions, the LEA allows one to correctly describe the rotational evolution of molecules exposed to laser pulses. Nevertheless this approach could not be satisfactory when very short and intense light pulses are considered. Indeed, the present technology [25] allows one to generate near-single-cycle intense light pulses [26]. Two new aspects appear simultaneously when such pulses are considered, namely, the larger peak intensity to which the molecule can be exposed without significant ionization and the rapid changes of the pulse envelope on the optical cycle scale. A large field peak is responsible for nonlinear distortion of the induced dipole moment, thus influencing the laser-molecule interaction. On the other hand the envelope approximation, based on the averaging of electric field oscillations during the interaction, could not describe effects related to fast changes of the pulse envelope on an optical cycle scale. Although these two aspects could have different weights, depending on the considered molecule and on the interaction parameters, they are inherent to the laser-molecule interaction in the regime of ultrashort pulse duration.

The aim of this work is to show that, in some peculiar cases and in the framework of classical electrodynamics, the interaction between an intense, ultrashort laser pulse and a molecule should be described including both the actual shape of the electric field of the pulse and the role of molecular hyperpolarizability. As a noticeable consequence, we will show that the inclusion of these terms implies the presence of carrier-envelope-phase effects in the classical dynamics of polar molecules driven by near-single-cycle light pulses.

The paper is organized as follows: in Sec. II a model for the classical description of molecular dynamics under the influence of an intense, few-optical-cycle laser pulse will be presented; the model will be developed in the regime of the nonresonant laser-molecule interaction. In Sec. III we will discuss the regimes in which the LEA deviates from the ac-

*Electronic address: stagira@fisi.polimi.it

tual molecular dynamics when the interaction with single ultrashort laser pulse is considered. Section IV will be devoted to the effects of hyperpolarizabilities on the classical molecular response induced by two-color laser pulses.

II. THEORETICAL MODEL

In this section a classical theoretical model for the laser-molecule interaction will be developed and compared to the linear envelope approximation. We will assume that the molecular response to an electric field is instantaneous and that the laser pulse frequency is far from resonances. In order to simplify our discussion, the molecules will be modeled as rigid rotors, thus assuming that molecular vibrations give negligible contribution to the rotational dynamics.

A. Laser-molecule interaction

Let us consider a molecule exposed to the electric field $\mathbf{E}(t)$ of an ultrashort laser pulse. In order to develop a general model, let us assume that the molecule has a dipole moment $\mathbf{d} = \mathbf{d}^{(0)} + \mathbf{d}_{\text{ind}}(\mathbf{E})$, where $\mathbf{d}^{(0)}$ is a permanent contribution and \mathbf{d}_{ind} is the contribution induced by the external field. Let us now consider the molecular equation of motion projected onto a Cartesian system $Oxyz$; fixed with respect to the molecule. Upon exposure to the laser pulse, the molecule experiences a torque $\boldsymbol{\tau} = \mathbf{d} \times \mathbf{E}$, which is related to the molecular angular momentum \mathbf{L} by the relation,

$$\boldsymbol{\tau} = \frac{d\mathbf{L}}{dt} + \boldsymbol{\omega} \times \mathbf{L}, \quad (1)$$

where $\boldsymbol{\omega}$ is the molecular angular velocity. In Eq. (1) we intentionally omit any dissipative term related to radiation emission and molecular collisions. Equation (1) can be written in terms of Cartesian components on the axes of $Oxyz$,

$$\tau_i = I_i^k \dot{\omega}_k + \epsilon_i^{jk} \omega_j I_k^l \omega_l, \quad (2)$$

where the Einstein convention for index summation is used and I_i^k is the molecular tensor of inertia, ϵ_i^{jk} is the permutation symbol, $\dot{\omega}_k = d\omega_k/dt$; all the indices can assume the values $\{x, y, z\}$. Expanding the molecular dipole moment as a function of the driving electric field components $E_k(t)$, one obtains

$$d_j = d_j^{(0)} + \alpha_j^l E_l + \beta_j^{lm} E_l E_m + \gamma_j^{lmn} E_l E_m E_n + \dots, \quad (3)$$

where α_j^l is the polarizability tensor of the molecule, β_j^{lm} and γ_j^{lmn} are the second and third-order hyperpolarizability tensors, respectively. From Eqs. (3) and (2), we obtain

$$\begin{aligned} \epsilon_i^{jk} (d_j^{(0)} + \alpha_j^l E_l + \beta_j^{lm} E_l E_m \\ + \gamma_j^{lmn} E_l E_m E_n + \dots) E_k = I_i^k \dot{\omega}_k + \epsilon_i^{jk} \omega_j I_k^l \omega_l. \end{aligned} \quad (4)$$

It is worth noting that the components of all the tensors are constant in the chosen Cartesian system, whereas the electric field and the angular velocity are functions of time. Introducing a fixed Cartesian system $OXYZ$, the motion of the molecule can be described in terms of the motion of the molecular frame $Oxyz$; this can be done using the three Euler angles

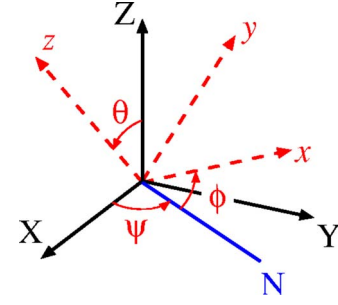


FIG. 1. (Color online) Euler angles θ , ψ , and ϕ , addressing the molecular frame $Oxyz$ with respect to the fixed frame $OXYZ$; N is the nodal axis obtained from the intersection between the XY and the xy planes.

θ , ψ , ϕ , as shown in Fig. 1. With the help of these new parameters, Eq. (4) can be rewritten as

$$\begin{aligned} \epsilon_i^{jk} (d_j^{(0)} + \alpha_j^l \Lambda_l^{\bar{p}} E_{\bar{p}} + \beta_j^{lm} \Lambda_l^{\bar{p}} \Lambda_m^{\bar{q}} E_{\bar{p}} E_{\bar{q}} \\ + \gamma_j^{lmn} \Lambda_l^{\bar{p}} E_{\bar{p}} \Lambda_m^{\bar{q}} E_{\bar{q}} \Lambda_n^{\bar{r}} E_{\bar{r}} + \dots) \Lambda_k^{\bar{h}} E_{\bar{h}} \\ = I_i^k \dot{\omega}_k + \epsilon_i^{jk} \omega_j I_k^l \omega_l, \end{aligned} \quad (5)$$

where $E_{\bar{k}}(t)$ are the electric field components in the fixed system $OXYZ$ and $\Lambda_k^{\bar{h}}(t)$ are functions relating the components in the fixed frame to those in the molecular frame $Oxyz$ [27]. Since the relation between $\boldsymbol{\omega}$ and the motion of the molecular frame is known [27], we obtain from Eq. (5) three equations describing the response of the molecule as a function of the applied electric field. The expressions for the quantities $\Lambda_k^{\bar{h}}$ and for the angular velocity $\boldsymbol{\omega}$ are reported in Appendix A.

B. Linear envelope approximation

The general model we have presented has been compared to the linear envelope approximation. In order to derive the equations for molecular evolution in the framework of the LEA, let us consider a polychromatic electric field written in a general form, as

$$E_{\bar{i}}(t) = \sum_{\lambda} \mathfrak{E}_{\lambda, \bar{i}}(t) \cos(\Omega_{\lambda} t - \eta_{\lambda, \bar{i}}), \quad (6)$$

where Ω_{λ} are the optical pulsations of the various spectral components of the pulse, $\mathfrak{E}_{\lambda, \bar{i}}(t)$ are the corresponding pulse envelope components projected onto the Cartesian axes XYZ and $\eta_{\lambda, \bar{i}}$ are the carrier-envelope phases corresponding to each axis. Inserting Eq. (6) into Eq. (5), neglecting the non-linear contributions and performing a temporal average over an optical cycle, one obtains the LEA for the dynamical equations,

$$\begin{aligned} \sum_{\lambda} \cos(\Delta \eta_{\lambda, \bar{h}, \bar{m}}) \epsilon_i^{jk} \alpha_j^l \Lambda_l^{\bar{h}} \Lambda_k^{\bar{m}} \mathfrak{E}_{\lambda, \bar{h}} \mathfrak{E}_{\lambda, \bar{m}} \\ = 2(I_i^k \dot{\omega}_k + \epsilon_i^{jk} \omega_j I_k^l \omega_l), \end{aligned} \quad (7)$$

where $\Delta \eta_{\lambda, \bar{h}, \bar{m}} = \eta_{\lambda, \bar{h}} - \eta_{\lambda, \bar{m}}$; in the derivation of Eq. (7), it was assumed that each component of the polychromatic pulse is

far from the others in the spectral domain and that the position of the molecule does not change during an optical cycle. It is worth noting that the phase difference $\Delta\eta_{\lambda,h,\bar{m}}$ is related to the polarization state of each spectral component of the optical pulse. According to the previous equation, permanent dipoles give no contribution to the molecular motion in the LEA. In the limit of very short driving pulses, the LEA can be further simplified to the so called *δ -kick approximation* [10,12]; in this case the final dynamical state of the molecule depends only on the pulse fluence and polarization, whereas it does not depend on the actual pulse duration (see Appendix B for details).

III. INTERACTION WITH A SINGLE LASER PULSE

In this section we will consider the interaction of molecules with an intense, ultrashort laser pulse. The theoretical model is illustrated through examples concerning the classical modelling of existing molecules. For the sake of simplicity, we omit details about the dynamics during the interaction and we limit the discussion to the final dynamical state of the molecule. The results will be represented by the acquired angular momentum, which is a conserved quantity after the interaction.

Moments of inertia, dipole moment, polarizability, and the first nonvanishing hyperpolarizability of the considered molecules were acquired from the literature [28–35]. The numerical solution of the dynamical equations was achieved using a standard Runge-Kutta algorithm. In the simulations it was assumed that the laser beam propagates in the fixed frame along the Y axis; the investigation was limited to molecules initially at rest. In order to perform realistic calculations, the driving pulse intensity was kept below the ionization threshold (which was fixed at the 5% of the overall population), according to the Ammosov-Delone-Krainov (ADK) model [36,37]. As a matter of fact, the ADK model must be considered only as a guideline for the choice of the maximum intensity, because it could work improperly for molecular species.

A. Analysis of linear rotor dynamics

We have first considered the case of a linear rotor exposed to an intense few-optical-cycle laser pulse, whose electric field is directed along the Z axis. In this case the rotor position is described by the angle θ with respect to Z; the angle ψ is constant during the interaction, whereas the evolution of ϕ can be neglected. We will neglect the role of hyperpolarizabilities, even though they can give a contribution to the rotor dynamics. In this case, Eq. (5) can be written as follows:

$$2I\ddot{\theta} + 2d_z E_Z(t) \sin \theta(t) + \Delta\alpha E_Z^2(t) \sin 2\theta(t) = 0, \quad (8)$$

where I is the moment of inertia, $\Delta\alpha = \alpha_{zz} - \alpha_{xx}$ is the polarizability anisotropy of the rotor, and $d_z = d_z^{(0)}$ is the permanent dipole moment. In order to write an analytical expression for the angular momentum acquired by the molecule after the interaction with the laser pulse, we approximate the sine functions in Eq. (8) with a Taylor expansion around the ini-

tial position θ_0 ; this approximation holds as far as the rotor undergoes small angular displacements during the laser pulse. Solving Eq. (8) at the zero-order of the Taylor expansion, plugging the result into the expansion up to the first order and integrating, one obtains the approximated angular momentum L_f acquired by the rotor after the interaction with the pulse,

$$L_f = L_0 + L_{\text{dip}} + L_{\text{pol}} + L_{\text{mix}}, \quad (9)$$

where

$$L_0 = -\frac{\Delta\alpha \sin 2\theta_0}{2} \int_{-\infty}^{\infty} E_Z^2(t) dt \quad (10)$$

is the angular momentum calculated assuming the rotor at rest during the interaction;

$$L_{\text{dip}} = \frac{d_z^2 \sin 2\theta_0}{2I} \int_{-\infty}^{\infty} dt E_Z(t) \int_{-\infty}^t dt' \int_{-\infty}^{t'} E_Z(\tau) d\tau \quad (11)$$

is the contribution related to the molecular dipole moment,

$$L_{\text{pol}} = \frac{\Delta\alpha^2 \sin 4\theta_0}{4I} \int_{-\infty}^{\infty} dt E_Z^2(t) \int_{-\infty}^t dt' \int_{-\infty}^{t'} E_Z^2(\tau) d\tau \quad (12)$$

is the additional contribution related to the polarizability and

$$L_{\text{mix}} = \frac{\Delta\alpha d_z}{I} \left[\frac{\cos \theta_0 \sin 2\theta_0}{2} \int_{-\infty}^{\infty} dt E_Z(t) \int_{-\infty}^t dt' \int_{-\infty}^{t'} E_Z^2(\tau) d\tau + \cos 2\theta_0 \sin \theta_0 \int_{-\infty}^{\infty} dt E_Z^2(t) \int_{-\infty}^t dt' \int_{-\infty}^{t'} E_Z(\tau) d\tau \right] \quad (13)$$

is the contribution related to the interplay between permanent dipole moment and polarizability. A negative angular momentum indicates that the rotor approaches the Z axis after the interaction.

In the framework of the envelope approximation, Eq. (8) is replaced by

$$2I\ddot{\theta} + \frac{\Delta\alpha \mathfrak{E}_Z^2(t)}{2} \sin 2\theta(t) = 0, \quad (14)$$

where $\mathfrak{E}_Z(t)$ is the envelope of the electric field $E_Z(t)$. According to the LEA, the angular momentum acquired by the molecule is

$$L^{\text{LEA}} = -\frac{\Delta\alpha \sin 2\theta_0}{4} \int_{-\infty}^{\infty} \mathfrak{E}_Z^2(t) dt \simeq -\frac{\Delta\alpha \mathcal{F} Z_v \sin 2\theta_0}{2}, \quad (15)$$

where $Z_v = \sqrt{\mu_0/\epsilon_0}$ is the vacuum impedance and $\mathcal{F} = \int_{-\infty}^{\infty} E_Z^2(t)/Z_v dt \simeq \frac{1}{2} \int_{-\infty}^{\infty} \mathfrak{E}_Z^2(t)/Z_v dt$ is the pulse fluence; in the previous equation we assumed the molecule at rest during the interaction (*δ -kick approximation*). It is worth noting that L^{LEA} is equal to the term L_0 ; thus the three remaining terms in Eq. (9) represent the discrepancy between the linear envelope approximation and the complete description of the rotor dynamics. We will focus the analysis on the two terms related to the dipole moment, because they are more interesting for the aim of this work. The results previously re-

ported can be easily interpreted in the spectral domain; in the following the Fourier transform of $E_Z(t)$ will be indicated as $\tilde{E}(\Omega)$.

1. Dipole term

According to the properties of the Fourier transformation, the dipole term L_{dip} can be written as

$$L_{\text{dip}} = -\frac{d_z^2 \sin 2\theta_0}{2I} \int_{-\infty}^{\infty} \frac{|\tilde{E}(\Omega)|^2 d\Omega}{\Omega^2 2\pi}. \quad (16)$$

In the case of a pulse with a spectral bandwidth $\Delta\Omega$ much smaller than the central frequency Ω_0 ($\Delta\Omega \ll \Omega_0$), Eq. (16) can be written as follows:

$$L_{\text{dip}} \approx -\frac{d_z^2 \mathcal{F} Z_v \sin 2\theta_0}{2I\Omega_0^2}, \quad (17)$$

where the Parseval theorem was used. The dipole correction to the angular momentum turns out to be proportional to the pulse fluences and to the dipole moment (thus, it is vanishing for nonpolar rotors) and it has the same sign of L_0 ; at constant fluence, the larger is the wavelength of the laser pulse, the larger is L_{dip} . Moreover, the dipole correction is smaller for heavier molecules. It is worth pointing out that the dipole correction holds also for multicycle laser pulses and can be very important for molecules with very large dipole moment. In order to show the relevance of this correction term, we considered the dynamics of a lithium hydride (HLi) molecule, initially at rest in the position $\theta_0 = \pi/4$, exposed to intense Gaussian laser pulses of different central frequencies; such a molecule was chosen owing to the very large dipole moment (5.88 D) and low inertia moment. Figure 2 shows the angular momentum correction factor, defined as

$$\Delta L = \frac{|L_f| - |L^{\text{LEA}}|}{|L^{\text{LEA}}|}; \quad (18)$$

ΔL is shown as a function of the pulse central frequency Ω_0 (filled dots). The pulse duration was $t_p = 5T$, where T is the optical period ($T = 2\pi/\Omega_0$). The calculated ΔL values are in excellent agreement with Eq. (17) (solid line in Fig. 2). As clearly shown in the figure, the correction factor increases upon decreasing the pulse central frequency, ranging from few percent in the visible up to 80% in the near infrared ($\Omega_0 \approx 5 \times 10^{14}$ rad/s).

For ultrabroadband laser pulses, Eq. (17) does not hold any more and Eq. (16) must be considered; one can show with simple argumentation that, for a fixed fluence and central frequency, a laser pulse with a larger bandwidth $\Delta\Omega$ induces a larger dipole term. Such finding is supported by numerical simulations, as reported in Fig. 3; the quantity ΔL was calculated for the same molecule at the pulse wavelength $\lambda = 1.6 \mu\text{m}$ as a function of the normalized pulse spectral bandwidth $\Delta\Omega/\Omega_0$, reported on the upper abscissa axis. The lower axis shows the corresponding pulse duration (only transform-limited pulses were considered). The results are shown as filled dots and are compared with the prediction of Eq. (16), shown as a solid line; values obtained using the

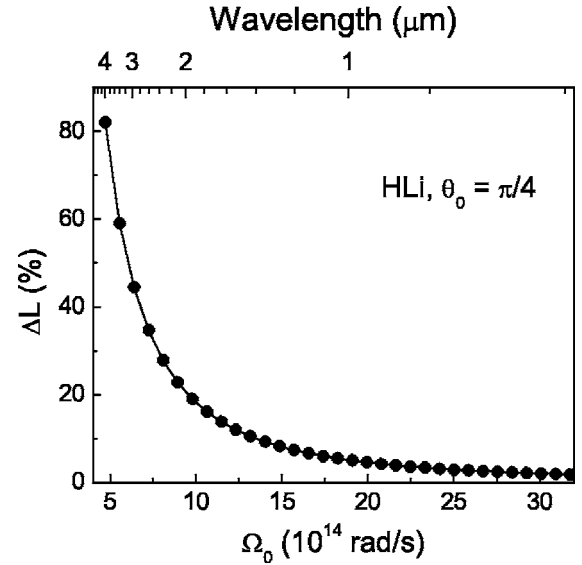


FIG. 2. Angular momentum correction factor for a HLi molecule exposed to an ultrashort laser pulse as a function of the central frequency of the pulse. Solid dots: calculation by full numerical simulations assuming a pulse fluence $\mathcal{F} = 2.1 \times 10^3 \text{ J/m}^2$ and a duration $t_p = 5T$; solid line: results predicted by the analytical approximation (17).

approximated relation (17) are also shown as dashed line for comparison. One can see that the dipole correction increases with the pulse bandwidth (i.e., increases for shorter durations, if transform-limited pulses are considered); an increase of more than 2% in the acquired angular momentum is obtained for single-cycle driving pulses. As a matter of fact, the spectral extension of the pulse is the only key factor; indeed, Eq. (16) does not depend on the spectral phase of the pulse.

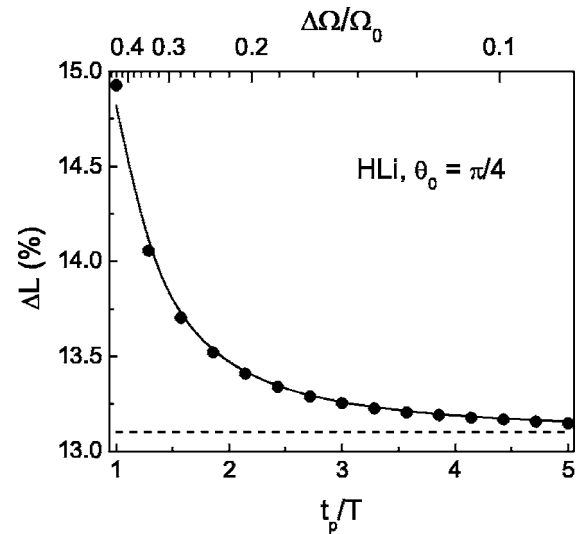


FIG. 3. Angular momentum correction factor for a HLi molecule as a function of the normalized bandwidth of the driving pulse. Filled dots: calculation by full numerical simulations assuming a pulse fluence $\mathcal{F} = 1.1 \times 10^3 \text{ J/m}^2$ and a central wavelength $\lambda = 1.6 \mu\text{m}$; solid line: results predicted by the analytical approximation (16); dashed line: prediction obtained according to Eq. (17).

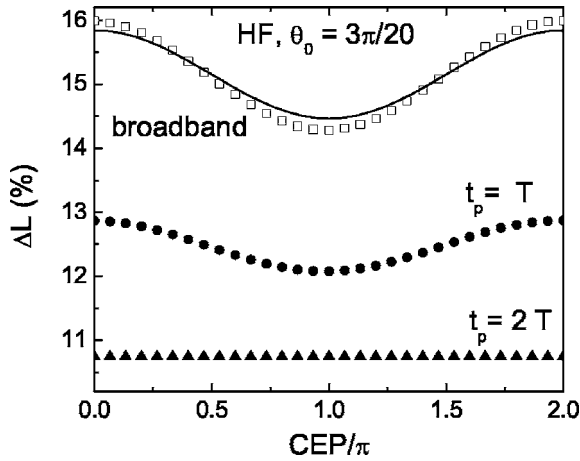


FIG. 4. Symbols: angular momentum correction factor for a HF molecule, calculated by full numerical simulations as a function of the CEP of the driving pulse, assuming a fluence $\mathcal{F}=1.9 \times 10^4 \text{ J/m}^2$ and a wavelength $\lambda=2.4 \mu\text{m}$ (filled triangles: two-cycles Gaussian pulse; filled dots: one-cycle Gaussian pulse; empty squares: ultrabroadband pulse). Solid line: results predicted by the analytical approximations (16) and (19).

Thus a similar result can be obtained inducing spectral broadening in multicycle driving pulses.

2. Mixed term

The term L_{mix} , that will be called mixed term hereafter, can be approximated by the following relation:

$$L_{\text{mix}} \approx - \frac{\Delta \alpha_d (3 \sin 3\theta_0 - \sin \theta_0)}{4I} \int_{-\infty}^{\infty} \frac{\tilde{E}^*(\Omega) A(\Omega) d\Omega}{\Omega^2 2\pi}, \quad (19)$$

where $A(\Omega) = \tilde{E}^* \tilde{E}$ is the autoconvolution of the pulse spectrum and \tilde{E}^* is the conjugate of \tilde{E} . It must be noted that, if the laser pulse has significant spectral components around Ω_0 , $A(\Omega)$ is not vanishing around $\Omega=0$ and $\Omega=2\Omega_0$. Thus, as far as the spectrum of the laser pulse is narrow, the mixed contribution will be negligible, because there will be negligible overlap between the two terms inside the integral in Eq. (19).

For ultrabroadband pulses (at least spanning one octave of the frequency range), a significant overlap could be observed; in such a case it can be shown that L_{mix} depends on the carrier-envelope phase (CEP) η of the driving laser pulse. Indeed, if the laser pulse is transform-limited, the function $A(\Omega)$ will show a vanishing phase around the spectral origin and a phase 2η around $2\Omega_0$; thus the overlap integral in Eq. (19) will depend on η .

In order to test such conclusion, we considered the dynamics of a HF molecule in the initial position $\theta_0=3\pi/20$, exposed to ultrashort pulses with central wavelength $\lambda=2.4 \mu\text{m}$ and fluence $\mathcal{F}=1.9 \times 10^4 \text{ J/m}^2$; the corresponding results are shown in Fig. 4. We choose this molecule because the higher ionization potential of HF (16.09 eV) with respect to HLi (7.9 eV) allows to expose the former to larger

fluences, with larger CEP effects. The quantity ΔL was calculated as a function of the pulse CEP for three different cases, namely, for single-cycle (filled dots) and two-cycles (filled triangles) Gaussian pulses and for an ultrabroadband transform-limited pulse (empty squares); in the latter case the pulse power spectrum, with super-Gaussian shape, has a normalized bandwidth $\Delta\Omega/\Omega_0=0.75$. One can see that the correction factor shows a negligible dependence on the CEP for two-cycle pulses, whereas a noticeable phase effect is present for shorter pulses; variations as large as 1% are observed for single-cycle pulses; an effect amounting to 2% is obtained for an ultrabroadband driving pulse. These findings confirm the presence of a CEP effect for pulses having a large spectral extension.

The numerical results were also compared to those obtained by the analytical approximations in the case of the ultrabroadband pulse (solid line in Fig. 4). The agreement between the two simulations is also very good in this case.

B. Ensemble of linear rotors

We have considered up to here the dynamics of a single rotor. Nevertheless it is useful to demonstrate that there is also a significant departure between the LEA and the actual molecular dynamics when a rotor ensemble is considered. Let us assume that an isotropic distribution of linear polar rotors, initially at rest, interacts with a laser pulse polarized along the Z axis. In order to represent the behavior of the ensemble, one can determine the so called classical alignment factor $\mathcal{A}(t) = \langle \cos^2 \theta(t) \rangle$, which measures the degree of alignment of the rotor ensemble along the Z axis. For an isotropic distribution of initial positions θ_0 , this quantity is given by

$$\mathcal{A}(t) = \frac{\int_0^\pi \cos^2 \theta(t, \theta_0) \sin \theta_0 d\theta_0}{2}; \quad (20)$$

the integration is performed between 0 and π in order to consider all the possible orientation of the polar rotors. Figure 5 shows the alignment factor of an ensemble of HF molecules, initially at rest, interacting with a 5-optical-cycle pulse. $\mathcal{A}(t)$ is constant and equal to 1/3 before the interaction; after the interaction, the alignment factor increases up to about 0.8 and then shows a damped oscillation around 0.5. It is worth noting that the prediction obtained according to the LEA (dashed line) differs from that obtained in the framework of the complete dynamical model (solid line). We ascribe this difference to the different angular distribution expected by the two models after the interaction.

C. Dynamics of nonlinear rotors

The study of the molecular dynamics of nonlinear rotors cannot be easily reduced to analytical treatment, because simultaneous variation of all three Euler angles during the interaction is expected; in such cases numerical simulations are required. As a typical example, we consider the interaction of a water molecule at rest (in the initial position $\theta_0=\psi_0=\phi_0=\pi/4$) with a laser pulse, linearly polarized along the Z axis.

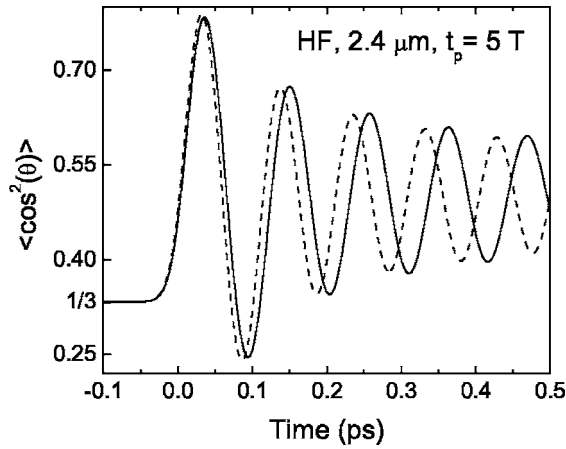


FIG. 5. Alignment factor of an ensemble of HF molecules interacting with a 5-optical-cycles pulse, with central wavelength $\lambda = 2.4 \mu\text{m}$, and fluence $\mathcal{F} = 7.5 \times 10^4 \text{ J/m}^2$ calculated according to the complete model (solid line) and to the envelope approximation (dashed line).

Owing to the complexity of the molecule dynamics, we calculated both the modulus and the Cartesian components of the angular momentum correction factor $\Delta\mathbf{L} = (\mathbf{L}_f - \mathbf{L}^{\text{LEA}})/|\mathbf{L}^{\text{LEA}}|$. The results are shown in Fig. 6 as a function of the central frequency Ω_0 for a 5-optical-cycle pulse.

The dynamics of the H_2O molecule is more complex with respect to a linear rotor; indeed not only the modulus, but also the direction of the final angular momentum changes with respect to that predicted by the envelope approximation. This effect is clearly shown by the changes in the Cartesian components of $\Delta\mathbf{L}$ in the laboratory frame. Indeed the angles ξ and ν formed by \mathbf{L}_f with the X and Y axes, respectively (symbols in the inset of Fig. 6) change with Ω_0 , whereas the

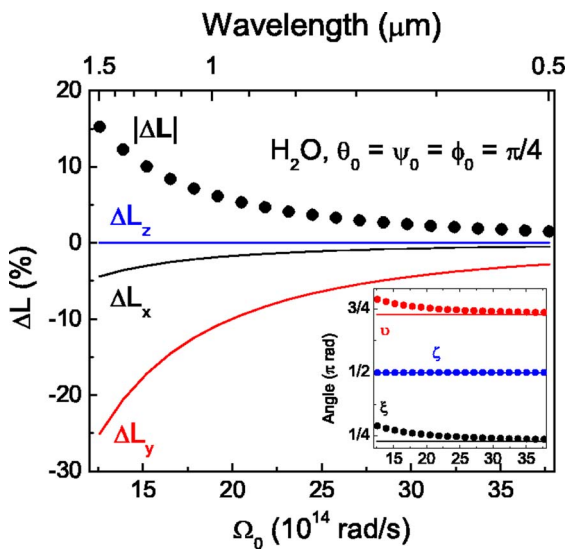


FIG. 6. (Color online) Angular momentum correction factor for a H_2O molecule calculated by full numerical simulations assuming a 5-optical-cycle pulse with a fluence $\mathcal{F} = 7 \times 10^3 \text{ J/m}^2$. Filled dots: modulus of $\Delta\mathbf{L}$; solid lines: Cartesian components. Inset: angles formed by \mathbf{L}_f (symbols) and \mathbf{L}^{LEA} (lines) with respect to the Cartesian axes.

angles formed by \mathbf{L}^{LEA} stay constant. It is worth noting that the angular momentum acquired by the molecule belongs to the XY plane irrespective to the pulse frequency; indeed the angle ζ formed by \mathbf{L}_f with the Z axis is always equal to $\pi/2$.

In conclusion, the classical LEA for polar molecule dynamics does not satisfactorily describe a few important effects related to the permanent dipole of the molecule. Such effects are more important for longer wavelength, lighter molecules and for large values of the permanent dipole. Moreover carrier-envelope phase effects, which have to be considered in the case of ultrabroadband pulses, are envisaged in the complete model, but are not present in the envelope approximation.

IV. MOLECULES INTERACTING WITH TWO-COLOR ULTRASHORT LASER PULSES

In this section we will consider the interaction of molecules with two-color ultrashort laser pulses. The discrepancy between the LEA and the complete model is related to the role of the molecular hyperpolarizabilities; such effect will be analyzed in detail for linear rotors and illustrated with the help of numerical simulations.

A. Analysis of linear rotor dynamics

We will limit the analytical treatment to the role of the second-order hyperpolarizability β in the dynamics of linear rotors; higher-order effects can be analyzed in a similar way. Let us assume that the only significant components of the hyperpolarizability are β_{zzz} , β_{zxx} , $\beta_{xxz} = \beta_{xzx}$ and the components obtained replacing x with y . Let us consider the interaction of the molecule with two simultaneous laser pulses with orthogonal polarization and central frequencies Ω_1 and $\Omega_2 = 2\Omega_1$, respectively; the overall electric field can be written as $\mathbf{E}(t) = F(t)\mathbf{u}_Z \cos(\Omega_1 t + \eta_1) + S(t)\mathbf{u}_X \cos(2\Omega_1 t + \eta_2)$, where \mathbf{u}_Z and \mathbf{u}_X are the unity vectors along the Z and the X axes, respectively. In order to simplify the analysis, we will assume that the molecule lies in the XZ plane and it is at rest during the interaction. The contribution of the molecular hyperpolarizability to the final angular momentum is given by

$$L^{(2)} = g(\beta, \theta_0) \int_{-\infty}^{\infty} F^2(t) S(t) \cos^2(\Omega_1 t + \eta_1) \cos(2\Omega_1 t + \eta_2) dt, \quad (21)$$

where

$$g(\beta, \theta_0) = (\beta_{zzz} - 2\beta_{xxz})(\cos^3 \theta_0 - 2 \sin^2 \theta_0 \cos \theta_0) + 3\beta_{zxx} \sin^2 \theta_0 \cos \theta_0. \quad (22)$$

Such contribution, which has to be summed to the angular momentum terms related to the linear polarizability and to the permanent dipole, is clearly due to a second-order non-linear effect, which is completely neglected by the linear envelope approximation. Assuming that the envelope of the electric field varies slowly with respect to the optical carrier, we can simplify Eq. (21) as follows:

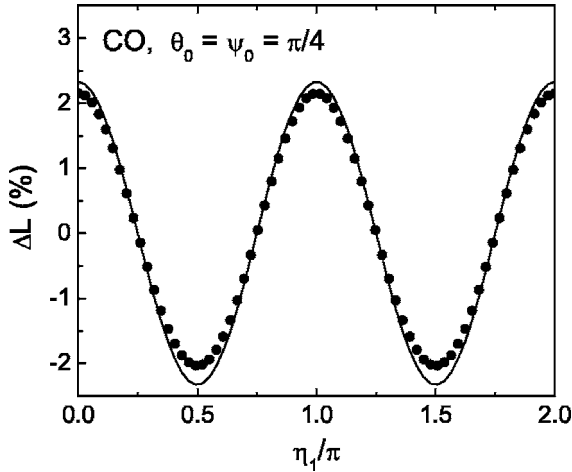


FIG. 7. Angular momentum correction factor for a CO molecule interacting with two-color laser pulses (see text); symbols: results of full numerical simulations as a function of the CEP η_1 ; solid line: prediction obtained according to Eq. (23).

$$L^{(2)} \simeq \frac{g(\beta, \theta_0)}{4} \cos(2\eta_1 - \eta_2) \int_{-\infty}^{\infty} F^2(t)S(t)dt. \quad (23)$$

Equation (23) shows a clear dependence on the CEP difference $\Delta\eta = 2\eta_1 - \eta_2$. In order to confirm such analytical result, we have performed numerical simulations for a CO molecule exposed to a bichromatic ultrashort laser pulse containing two components: the former (at 800 nm, with time duration of 5 optical cycles), is polarized along the Z axis; the latter, (at 400 nm, with time duration of 10 optical cycles) is polarized along the X axis. The two pulses impinge on the molecule simultaneously; each pulse has a fluence $\mathcal{F} = 7 \times 10^3 \text{ J/m}^2$; the initial position of the molecule, assumed at rest, was set to $\theta_0 = \pi/4$. The angular momentum correction factor $\Delta L = (|\mathbf{L}_f| - |\mathbf{L}^{\text{LEA}}|) / |\mathbf{L}^{\text{LEA}}|$ obtained by simulations is reported in Fig. 7 as a function of the phase η_1 of the 800-nm pulse; the phase of the second harmonic pulse was set to the constant value $\eta_2 = 0$. As clearly shown by the figure, the nonlinear contribution to the final angular momentum is phase-dependent; it is worth noting that the prediction obtained according to Eq. (23) (solid line in Fig. 7), is in very good agreement with the numerical simulations (filled dots). Indeed, the correction terms of Eqs. (11) and (13) have negligible role in this case, owing to the large inertia and low dipole moment of CO. Thus the main correction term is related to the second-order hyperpolarizability.

B. Dynamics of nonlinear rotors

In the framework of an analytical treatment, it is difficult to predict the nonlinear effects induced on the dynamics of nonlinear rotors. In the case of second-order effects, one could assume that a phase dependence, similar to that previously seen, also holds for nonlinear molecules. Nevertheless more complicated effects can also be envisaged. In order to provide an example of such effects, let us consider the CH_4 molecule. The methane molecule shows a tetrahedral group symmetry, corresponding to isotropic polarizability and iner-

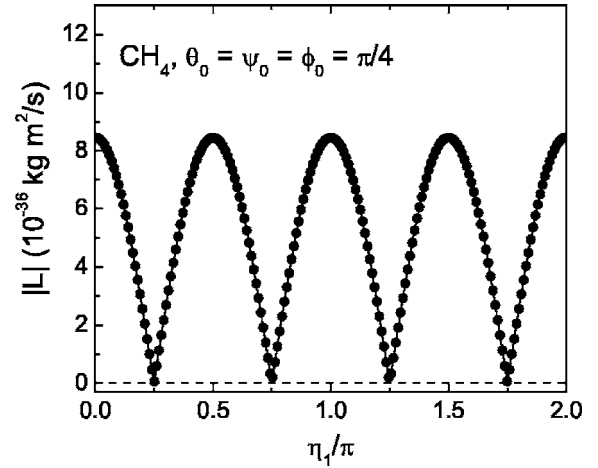


FIG. 8. Symbols: angular momentum of a CH_4 molecule calculated by full numerical simulations as a function of the CEP η_1 in the case of a two-color excitation (see text); solid line: fitting according to the $|\cos \Delta\eta|$ function; dashed line: prediction obtained according to the linear envelope approximation.

tia moment tensors [33]. It can be shown that, in a reference system $Oxyz$ whose axes are directed along the sides of a cube containing the methane tetrahedron, the significant components of the second-order hyperpolarizability are given by [38] $\beta_{lmn} = \beta(i_l j_m k_n + i_l j_n k_m + i_m j_l k_n + i_m j_n k_l + i_n j_l k_m + i_n j_m k_l)$, where \mathbf{i} , \mathbf{j} , and \mathbf{k} are the unit vectors along the x , y , z axes. We would like to investigate whether, in the framework of classical electrodynamics, the methane molecule could be rotationally excited by few-cycle laser pulses. If we limit our analysis to the linear envelope approximation, the answer is negative; owing to the isotropic nature of α_{ij} , the induced dipole in methane is always parallel to the pulse electric field; thus the torque induced in the molecule is always vanishing. A different result is obtained when the second-order hyperpolarizability is taken into account. We performed the numerical calculations using the same bichromatic laser pulse considered in the previous simulation. The methane molecule was assumed at rest, with the three Euler angles initially set to $\pi/4$. Figure 8 shows the quantity $|\mathbf{L}_f|$ as a function of η_1 , assuming $\eta_2 = 0$. In the linear envelope approximation, the induced dipole should stay parallel to the field. Thus a molecule initially at rest would stay in the same position after the interaction with the laser pulses and the corresponding angular momentum would be vanishing. Indeed, this is the prediction obtained by simulations according to the LEA (dashed line in Fig. 8). The results obtained with the complete numerical model (shown as symbols) are different; the molecule can be rotationally excited by the bichromatic laser pulse. Moreover the acquired angular momentum depends on the quantity $\Delta\eta = 2\eta_1 - \eta_2$. It is worth noting that the result can be satisfactorily fitted by the relation $|\mathbf{L}_f| \propto |\cos \Delta\eta|$ (shown as a solid line in the figure). This unsuspected behavior is entirely ascribed to the interaction between the field at 400 nm and the second-harmonic nonlinear dipole induced in the molecule by the field at 800 nm. In order to prove this assumption, we repeated the same simulation “switching off” the nonlinear term in the complete numerical model. The results (not shown) agree completely with those obtained by the LEA.

V. CONCLUSIONS

The classical rotational dynamics of molecules interacting with laser pulses is very often satisfactorily described by the linear envelope approximation (LEA). In this work we have shown that, in the framework of classical electrodynamics, the LEA sometimes fails in the prediction of the molecular state after the interaction. We demonstrated that, in those cases, the interaction between an intense, few-optical-cycle laser pulse and a molecule should be described including the actual shape of the pulse electric field and the role of molecular hyperpolarizability. In particular, we proved that it is not always possible to neglect the oscillating nature of light when the classical interaction of a polar molecule with a laser pulse is taken into account; we also observed a failure of the LEA in the modelling of rotational dynamics when the molecule interacts with bichromatic fields, owing to the contribution of the molecular hyperpolarizability.

We point out that an exhaustive description of laser-molecule interaction can be obtained only in the framework of quantum mechanics. Nevertheless many quantum models available in the literature are based on Hamiltonians with an interaction term determined in the framework of the LEA. The failure of this approximation in the classical description, though limited to some cases, calls for further investigations in the framework of quantum theories.

ACKNOWLEDGMENTS

This work was partially supported by the European Community's Human Potential Programme under Project No. MRTN-CT-2003-505138 (XTRA), and by Istituto Nazionale per la Fisica della Materia (INFN) under the project SPARC.

APPENDIX A: EULER ANGLES AND COORDINATE TRANSFORMATION

The molecular frame $Oxyz$ can be addressed with respect to the fixed frame $OXYZ$ through the Euler angles (θ, ψ, ϕ) [27], as shown in Fig. 1. The angle θ is also called *nutation* of the axis z ; the angle ψ is the *precession* of z , whereas ϕ is the *rotation* about z . The components v_i , with respect to the molecular frame, of a given vector \mathbf{v} can be written as follows:

$$v_i = \Lambda_i^{\bar{h}} v_{\bar{h}}, \quad (\text{A1})$$

where $v_{\bar{h}}$ are the components of \mathbf{v} in the fixed frame. The transformation matrix obeys the relation $\Lambda_i^{\bar{h}} = \bar{\mathbf{u}}_{\bar{h}} \cdot \mathbf{u}_i$, where $\bar{\mathbf{u}}_{\bar{h}}$ are the unity vectors of the XYZ axes and \mathbf{u}_i those of the xyz axes. $\Lambda_i^{\bar{h}}$ can be expressed as a function of the Euler angles according to the following relation [27]:

$$\Lambda_i^{\bar{h}} = \begin{bmatrix} -\sin \phi \cos \theta \sin \psi + \cos \phi \cos \psi & \cos \psi \sin \phi \cos \theta + \cos \phi \sin \psi & \sin \theta \sin \phi \\ -\cos \phi \cos \theta \sin \psi - \cos \psi \sin \phi & \cos \phi \cos \psi \cos \theta - \sin \phi \sin \psi & \sin \theta \cos \phi \\ \sin \theta \sin \psi & -\sin \theta \cos \psi & \cos \theta \end{bmatrix}. \quad (\text{A2})$$

The angular speed of the molecule can be projected onto the axes of the molecular frame and expressed again in terms of the Euler angles [27],

$$\begin{aligned} \omega_x &= \dot{\theta} \cos \phi + \dot{\psi} \sin \theta \sin \phi, \\ \omega_y &= -\dot{\theta} \sin \phi + \dot{\psi} \sin \theta \cos \phi, \\ \omega_z &= \dot{\phi} + \dot{\psi} \cos \theta. \end{aligned} \quad (\text{A3})$$

Thus, all the quantities appearing in Eq. (5) are functions of the Euler angles and of their temporal derivatives.

APPENDIX B: δ -KICK APPROXIMATION

Let us assume that the envelope of the laser pulse can be written as

$$\mathfrak{E}_{\lambda, \bar{h}}(t) = A_{\lambda, \bar{h}} \delta(t), \quad (\text{B1})$$

where $\delta(t)$ is the Dirac delta function; it is worth noting that, in the framework of this approximation, the pulse fluence is

fixed by the values of the quantities $A_{\lambda, \bar{h}}$, whichever the actual pulse duration is. Substituting Eq. (B1) in Eq. (7) and performing an integration over a very short time interval containing the driving pulse, one obtains

$$\begin{aligned} \sum_{\lambda} \cos(\Delta \eta_{\lambda, \bar{h}, \bar{m}}) \epsilon_i^k \alpha_j^l \Lambda_i^{\bar{h}} \Lambda_k^{\bar{m}} A_{\lambda, \bar{h}} A_{\lambda, \bar{m}} \\ = 2I_i^k (\omega_k^+ - \omega_k^-), \end{aligned} \quad (\text{B2})$$

where ω_k^- and ω_k^+ are the components of the angular velocity before and after the pulse. For a fixed polarization state and fluence of the laser pulse and for a given initial position of the molecule, the left-hand side of Eq. (B2) is a constant vector. We can thus conclude that, as far as the pulse duration is very short, the dynamical state of the molecule expected by the δ -kick approximation at the end of the interaction depends only on the pulse fluence and polarization, whereas it does not depend on the actual pulse duration.

- [1] P. Debye, *Polar Molecules* (Chemical Catalog, New York, 1929).
- [2] A. C. Newell and J. V. Moloney, *Nonlinear Optics* (Addison-Wesley, Redwood City, 1992).
- [3] R. W. Boyd, *Nonlinear Optics* (Academic, San Diego, 1992).
- [4] J.-L. Déjardin, *Phys. Rev. E* **52**, 4646 (1995).
- [5] B. A. Zon, *Eur. Phys. J. D* **8**, 377 (2000).
- [6] G. R. Kumar, P. Gross, C. P. Safvan, F. A. Rajgara, and D. Mathur, *Phys. Rev. A* **53**, 3098 (1996).
- [7] L. D. Landau and E. M. Lifshitz, *Quantum Mechanics: Non-Relativistic Theory* (Pergamon, Oxford 1977).
- [8] J. H. Van Vleck, *Phys. Rev.* **30**, 31 (1927).
- [9] M. Leibscher, I. Sh. Averbukh, P. Rozmej, and R. Arvieu, *Phys. Rev. A* **69**, 032102 (2004).
- [10] M. Leibscher, I. Sh. Averbukh, and H. Rabitz, *Phys. Rev. A* **69**, 013402 (2004).
- [11] B. A. Zon and B. G. Katsnel'son, *Sov. Phys. JETP* **42**, 595 (1976).
- [12] T. Seideman, *Phys. Rev. Lett.* **83**, 4971 (1999).
- [13] H. Stapelfeldt and T. Seideman, *Rev. Mod. Phys.* **75**, 543 (2003).
- [14] C. H. Lin, J. P. Heritage, and T. K. Gustafson, *Appl. Phys. Lett.* **19**, 397 (1971).
- [15] M. Wittmann, A. Nazarkin, and G. Korn, *Opt. Lett.* **26**, 298 (2001).
- [16] R. A. Bartels, T. C. Weinacht, N. Wagner, M. Baertschy, C. H. Greene, M. M. Murnane, and H. C. Kapteyn, *Phys. Rev. Lett.* **88**, 013903 (2002).
- [17] B. Friedrich and D. Herschbach, *Phys. Rev. Lett.* **74**, 4623 (1995).
- [18] R. Velotta, N. Hay, M. B. Mason, M. Castillejo, and J. P. Marangos, *Phys. Rev. Lett.* **87**, 183901 (2001).
- [19] M. Lein, P. P. Corso, J. P. Marangos, and P. L. Knight, *Phys. Rev. A* **67**, 023819 (2003).
- [20] C. Vozzi, F. Calegari, E. Benedetti, J.-P. Caumes, G. Sansone, S. Stagira, M. Nisoli, R. Torres, E. Heesel, N. Kajumba, J. P. Marangos, C. Altucci, and R. Velotta, *Phys. Rev. Lett.* **95**, 153902 (2005).
- [21] F. J. Aoiz, B. Friedrich, V. J. Herrero, V. Sáez Rábanos, and J. E. Verdasco, *Chem. Phys. Lett.* **289**, 132 (1998).
- [22] D. M. Villeneuve, S. A. Aseyev, P. Dietrich, M. Spanner, M. Yu. Ivanov, and P. B. Corkum, *Phys. Rev. Lett.* **85**, 542 (2000).
- [23] I. V. Litvinyuk, Kevin F. Lee, P. W. Dooley, D. M. Rayner, D. M. Villeneuve, and P. B. Corkum, *Phys. Rev. Lett.* **90**, 233003 (2003).
- [24] P. W. Dooley, I. V. Litvinyuk, Kevin F. Lee, D. M. Rayner, M. Spanner, D. M. Villeneuve, and P. B. Corkum, *Phys. Rev. A* **68**, 023406 (2003).
- [25] M. Nisoli, S. De Silvestri, and O. Svelto, *Appl. Phys. Lett.* **68**, 2793 (1996).
- [26] B. Schenkel, J. Biegert, U. Keller, C. Vozzi, M. Nisoli, G. Sansone, S. Stagira, S. De Silvestri, and O. Svelto, *Opt. Lett.* **28**, 1987 (2003).
- [27] L. D. Landau and E. M. Lifshitz, *Mechanics* (Pergamon, Oxford, 1976).
- [28] E. A. Moelwyn-Hughes, *Physical Chemistry* (Pergamon, Oxford, 1978).
- [29] Y. Tu and A. Laaksonen, *Chem. Phys. Lett.* **329**, 283 (2000).
- [30] O. Christiansen, J. Gauss, and J. F. Stanton, *Chem. Phys. Lett.* **305**, 147 (1999).
- [31] M. Gussoni, M. Rui, and G. Zerbi, *J. Mol. Struct.* **447**, 163 (1998).
- [32] T. Hamada, *Chem. Phys.* **211**, 171 (1996).
- [33] A. D. Buckingham and G. C. Tabisz, *Opt. Lett.* **1**, 220 (1977).
- [34] G. L. Bendazzoli, A. Monari, V. Magnasco, G. Figari, and M. Rui, *Chem. Phys. Lett.* **382**, 393 (2003).
- [35] L. Warton, L. P. Gold, and W. Klemperer, *J. Chem. Phys.* **33**, 1255 (1960).
- [36] M. V. Ammosov, N. B. Delone, and V. P. Krainov, *Zh. Eksp. Teor. Fiz.* **91**, 2008 (1986); [*Sov. Phys. JETP* **64**, 1191 (1986)].
- [37] R. C. Weast (editor), *CRC Handbook of Chemistry and Physics* (CRC Press, West Palm Beach, 1979).
- [38] A. D. Buckingham, *Adv. Chem. Phys.* **12**, 107 (1967).